



Response of Atlantic salmon in flexible sea cages to waves and currents: Measurements at farm-level and modeling

Pascal Klebert^{*}, Biao Su, Oscar Nissen, Bjarne Kvæstad

SINTEF OCEAN, Department of Aquaculture, Trondheim, Norway

ARTICLE INFO

Keywords:

Sea cage
Waves
Currents
Echosounder
Environmental parameters
Modeling

ABSTRACT

The shift towards salmon farming in more exposed locations has been an industry-wide trend for the last decade. Moving fish farms to locations with high water currents and waves can improve production by providing more stable temperatures and water quality, as well as reducing the negative environmental impacts of fish farming. This study investigates how waves affect the behavior of salmon from the same group, reared at different locations within a fish farm in standard circular sea cages. Using echosounders, DO (dissolved oxygen), temperature sensors and ADCP (Acoustic Doppler Current Profiler), we show that salmon avoid waves, swim below them and maintain their normal behavior. We also show that salmon behavior is related to the exposure of the cage, in the farm layout, to waves and currents. An integrated numerical model of fish and flexible sea cages is used to simulate the fish behavior under waves and currents and it able to reproduce the observed fish distributions in general.

1. Introduction

The salmon aquaculture industry has experienced enormous evolution and growth in Norway. Initially, most salmon farms were located in fjords or bays with low exposure to currents or waves. Over the past decade, the industry has moved to more high-energy sites, thereby increasing the exposure of cage systems to high currents and waves. Many stakeholders in the industry argue for moving fish farms to more exposed locations due to near-shore area conflicts, possible avoidance of sea lice and less challenges with farm emissions (Bjelland et al., 2015). Individual farms can also hold more fish in exposed locations (McIntosh et al., 2022). The combined effect of these two trends, larger farms in more exposed locations, has substantially increased the need for a better understanding of fish behavior and physiology due to high currents and waves (Morro et al., 2021). High current speeds have some distinct benefits for fish farming, such as providing better access to more consistent water quality, rapid dispersion of wastes and reduced benthic impacts (Holmer, 2010). The behavior of Atlantic salmon in sea cages has been thoroughly studied (Johansson et al., 2006; Elliott and Elliott, 2010; Oppedal et al., 2011) and temperature and salinity were found to be the main drivers of salmon behavior. The swimming speed of Atlantic salmon (Remen et al., 2016; Solstorm et al., 2016; Hvas and Oppedal, 2017) has been investigated mainly in a swim tunnel and a pushed cage

(Hvas et al., 2017). The effect of water current on the behavior of Atlantic salmon has also been studied in sea cages and it was found that at high current velocities, the salmon switched from normal circular movement to a group structure in which all the fish kept stations at fixed positions, swimming against the current (Johansson et al., 2014; Hvas et al., 2021). The behavior of farmed salmon is also affected by deformation of the cage when subject to currents (Klebert et al., 2013, 2015) and waves (Endresen and Klebert, 2020).

Field studies were recently conducted on the effects of waves on fish behavior and welfare (Johannesen et al., 2022, 2020). These studies demonstrated that the main effects of waves and currents on salmon behavior relate to how they reduce the space available for the fish. The salmon actively chose to occupy the parts of the cage that were exposed to high currents but avoided the sea surface in high waves. It was also found that when the deformation of the cage was too large due to high currents, the salmon were forced to move towards the surface even if high waves occur, in order to avoid contact with the lower parts of the net of the cage. These field measurements were performed with sea cages in shallow locations and so with a limited depth of the cage. No similar studies have been performed with deeper and conventional circular cages; these are investigated in this paper.

Traditionally, the characterization of wave exposure at Norwegian fish farms has been based on a certain range distribution of significant

^{*} Corresponding author.

E-mail address: pascal.klebert@sintef.no (P. Klebert).

wave heights H_s and peak wave periods T_p . A similar classification describes current exposure. The regulatory authorities, in collaboration with the aquaculture industry, have gained experience and insight into the importance of customized equipment in terms of structural strength and reliability, and through this knowledge a technical standard, NS9415, has been developed by Standard Norway (Standard Norge, 2009).

Lader et al. (2017) proposed a classification method with respect to wind and waves by using long-term wind data and fetch length to classify all Norwegian aquaculture sites. None of the 1070 studied sites were exposed to class E (Extreme), whereas around 18% of the sites experienced wave conditions characterized as C (Medium) or D (High) at least once a year. However, the authors emphasized that their study did not take in account swell, exposure to which can greatly increase the 1-year H_s and 50-year H_s for a site. Waves are separated into swell, wind-generated waves and waves scatter due to nearby topography. Hence, wave conditions at near-shore aquaculture sites can be quite complex. There can also be significant local spatial variations at a site, causing different levels of exposure at different parts of the farm. Small islands, reefs and local bathymetry affect the local wave conditions at near-shore sites through refraction, diffraction and scatter effects, which cause wave conditions to vary considerably at a site.

2. Materials and methods

2.1. Field site

The measurements were performed at a salmon farm at the full-scale SINTEF research facility located at Tristeinen (Latitude: 63°52'0.01", Longitude: 9°37'0.01"), which is an island in the region of Trøndelag, Norway (Figs. 1 and 2). The site is exposed to currents and large waves during the winter. The cages were laid out in a double straight line along the island, which is oriented 17° to the north-south axis.

The island creates a shield against high currents and waves from a northwesterly direction. Despite not being fully tidal, the currents flow, alternating between northbound and southbound directions. The location of the farm is quite deep (55–65 m) and, due to the layout of the farm and the hydrodynamic conditions, the side closest to the island is more sheltered than the other sides. Depending on the wind direction, waves enter the strait either from the southwest or the northeast. Three cages were selected in this study and numbered 1, 8 and 10. According to the classification (Table 1) and historical data, this site is classified as class A (small) for currents and as class C (medium) for waves. In the present study, the measured maximum wave heights (H_{max}) are close to 3 m (Fig. 5) and significant wave heights are close to 2 m.

2.2. Experimental design and measurements (Table 2)

- A SeaWatch Midi buoy from Fugro OCEANOR was located around 250 m to the southeast of the farm with a northerly current flow. This buoy is a moored surface buoy with instruments that collect weather and ocean data, including air temperature, sea surface temperature, sea temperature and salinity, wave statistics, wind speed/direction and current flow velocity. The instrument used for wave heights and periods measurements was the OCEANOR Wavesense wave sensor, which is designed for operation in remote locations. It is an inertial motion sensor that uses accelerometers, angular rate sensors. The accuracy of the sensor is given as ± 10 cm. Time series of three-dimensional buoy motion and wave parameters such as height, period, direction are the sensor outputs. Waves were measured from the buoy every hour during a 17.5-minute burst. The current measurements were performed with a sampling rate of 1 Hz over an ensemble two intervals of 10 minutes (600 samples) with output once every hour. This yielded a time series of hourly (10 min average) current velocities and directions. The speed range was 0–300 cm/s, discretized by 256 points (bin size 1.2 cm/s), and the depth cell size was 3 m. The data were post-processed internally on the buoy before being sent ashore every hour.
- To measure the vertical distribution of salmon in the water column, each cage was instrumented with an echosounder system comprising three transducers placed along the diameter in a south-north direction. The two transducers on each side were located at a depth of 12 m while the one in the middle was located at a depth of 14–15 m: all three transducers measured in an upward direction at a sampling rate of 4 s (Fig. 3).
- DO, salinity and temperature sensors were located at three different depths: 3, 5 and 12 m. All cages at the farm used skirts in the first seven meters below the ocean's surface. Skirts were used as a mitigation measure against seal ice infestation (Stien et al., 2018) as they offered protection from sea lice copepods, which are believed to be mainly located in the upper part of the water column. The DO and temperature sensor that were used in the cages are from Aanderaa, while the salinity sensors and DO sensors at the reference point outside the farm were wireless sensors from Innovasea (Table 1). Dissolved oxygen was measured every five minutes and the temperature and salinity every 10 min (Fig. 3).

2.3. Fish group and welfare scoring

Fish in the three cages (M1, M8, M10) came from the same group and were checked before and after being transported at sea in August 2020 with a weight ranging from 60 g to 132 g. During the measurements, regular welfare checks using the usual Operational Welfare Indicator registrations (Noble et al., 2018) were performed by fish health services

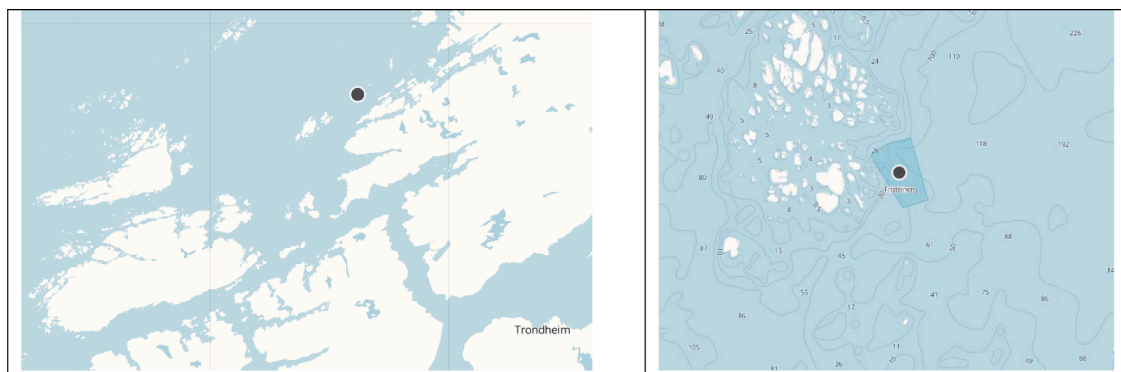


Fig. 1. Study site. The map shows the precise location of the farm and study cage in close up, as well as zoomed out maps of the general location in relation to the surrounding islands with 10 m depth contours. Map reprinted from Barentswatch (www.barentswatch.no).

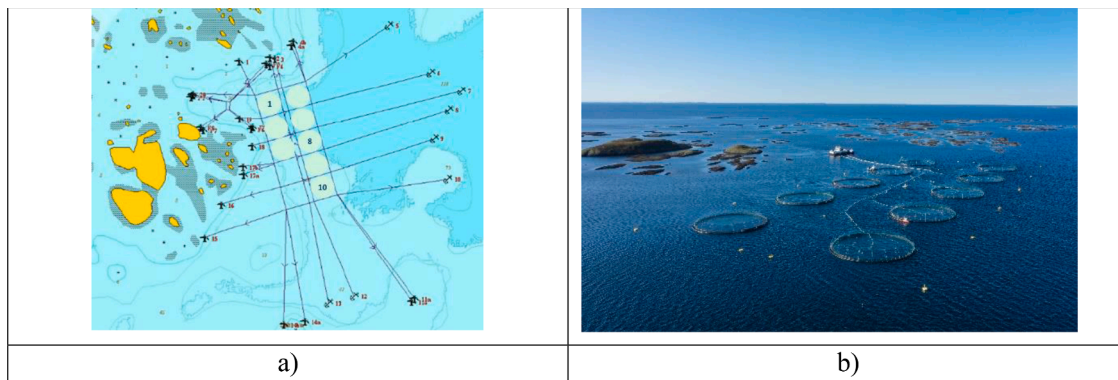


Fig. 2. (a) Layout of the cages inside the farm. Cages 1, 8 and 10 were studied (b) Aerial view of the farm.

Table 1
Aquaculture site classes with respect to exposure.

Wave class	H_s [m]	T_p [s]	Degree of exposure	Current class	V_c [m/s]	Degree of exposure
A	0.0–0.5	0.0–2.0	Small	a	0.0–0.3	Small
B	0.5–1.0	1.6–3.2	Moderate	b	0.3–0.5	Moderate
C	1.0–2.0	2.5–5.1	Medium	c	0.5–1.0	Medium
D	2.0–3.0	4.0–6.7	High	d	1.0–1.5	High
E	>3.0	5.3–18.0	Extreme	e	>1.5	Extreme

every two to three weeks when the weather permitted. All fins and eyes were checked and were scored (between 0 and 3) each time for around 20 fish per cage. The data show that all the indicators were below 1.5 (this value was only recorded once when checking the most exposed cage), which indicates good fish welfare during these measurements.

2.4. Data collection and processing

2.4.1. Environmental data

Data from the buoy were transmitted on an hourly basis. Wave data were processed internally, while current data were mean values for two 10-minute "bursts" every hour at different depths ranging from 5 m to 50 m with a three-meter cell height. The current and wave data collected from the buoy were initially screened and analyzed in order to detect the time intervals with high waves. From these time intervals, all the remaining data from DO, temperature and echosounders were analyzed. Instances of wave heights higher than 1 m were regarded as high. In this paper, only the analyzed data during these time intervals have been reported. As data from DO, temperature and salinity sensors were collected at a higher frequency than the wave data (hourly), once a time point with high waves had been detected, the DO, temperature and salinity data recorded during an interval of ± 20 min around the

detected time for high waves were associated with this specific wave case. All data were first filtered in order to consider only realistic values. Eliminating outliers and averaging can be useful for reducing the effect of random measurement errors. The outlier detection algorithm was provided by the Matlab R2022 library (MathWorks, Inc. Natick, Massachusetts, USA).

To assess the strength of association and correlation between the filtered dissolved oxygen sensor datasets, a statistical analysis was performed. The correlation was graded in terms of the Spearman rank order coefficient where, for an existing monotonic relationship, the coefficient quantifies the strength of the relationship between two variables. In comparison to other commonly used correlation methods, the Spearman's coefficient is marginally favored for datasets that contain at least one identical value (Puth et al., 2015). After confirming numerous identical values between all the datasets, correlation coefficient values were found using Spearman algorithm from the MATLAB library ("MATLAB and Statistics Toolbox Release 2020, The MathWorks, Inc., Natick, Massachusetts, United States," n.d.). To ensure all datasets had the same number of cases for each variable, all the dissolved oxygen datasets were synchronized to the dataset with the least number of datapoints. The sensor with the smallest sample size resulted in 1810 datapoints, used during the correlation analysis.

2.4.2. Echosounder data processing

The echosounder data were processed using Python 3.6 (Van Rossum and Drake, 2009), NumPy (Harris et al., 2020), Pandas (McKinney, 2010) and pyEcholab (Wall et al., 2018), which is a python package for reading, writing, processing and plotting data from Simrad/Kongsberg sonar systems. Using these modules, the echosounder data, represented in S_v (acoustic backscattering strength), were compiled to a data series containing three time series per echosounder. (i) Estimated distance from echosounder to water surface, (ii) 50th percentile fish population position relative to the water surface and (iii) average acoustic

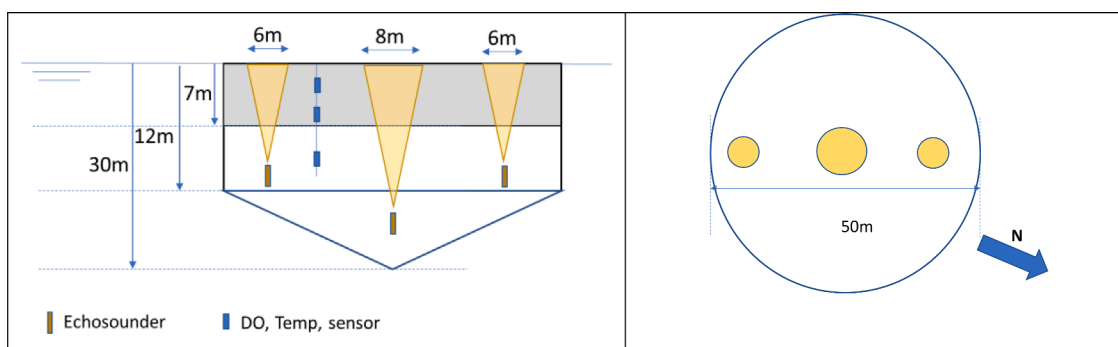


Fig. 3. Measurements and sensor setup. Top and side view of the sensor setup used inside the studied cages with the location of echo sounders (yellow circles and cones show the viewing area of the echo sounders but not the exact dimensions), DO, temp, sensors.

backscattering strength, calculated from echo sounder to water surface.

The estimated distance to water surface was derived by finding a region of interest (ROI) per echosounder data sample (lasting 24 h); the ROI was defined by summing across all bins along the time axis, then derived along the depth axis to find the area with the most distinct edge (highest rate of change). Within this ROI, the bin with the strongest signal was selected as an estimated distance to surface value. A sliding window of 20 samples wide (80 s) from echosounder to the estimated water surface was defined. For each iteration of the sliding window, the bins were summed along the time axis, generating a curve similar to a normal distribution curve; the 50th percentile fish population was found by integrating this curve from the water surface toward the echo sounder until 50% of the total area below the curve was reached. These data series were calculated for each echosounder channel and stored in a Pandas "dataframe" (McKinney, 2010) for efficient data lookup and manipulation. The estimated data points are compared to the raw data in Fig. 4.

Using the estimated surface and 50th percentile position data with the wave data from the buoy, the fish position data are presented in two ways: (1) a vertical distribution heat map compared to wave height and (2) a bar plot in to wave height.

- (1) For each datapoint in the wave height dataset, the S_v data measured ± 30 min from the wave height data point were found, the S_v data were corrected in terms of the estimated surface data and added together in wave height bins; each bin was divided by the number of samples in each bin order to generate an average distribution heat map, see Fig. 11.
- (2) 50th percentile data were binned in predetermined wave height bins in which the mean and standard deviation were calculated and represented using an bar plot, see Fig. 12.

3. Results

3.1. Wave, wind and current flow measurements

The data reported in this paper are from the months of October 2020 to April 2021, during which time high wave heights were measured (Fig. 5). Both maximum wave height (H_m) and significant wave height (H_s : mean wave height of the highest third of the waves) are represented. Missing data from the end of January to the beginning of February is due to an incident on the buoy during this period.

The wave heights and wave period data are shown in Fig. 6. Most of the wave periods lasted between 5 and 6 s. In the subsequent rose diagrams, the wave direction and current flow direction have been plotted based on the same definition, referring to the direction in which the current flows and the waves move.

The current velocity and direction are represented at two depths (5–11 m) in Fig. 7. It shows that the site is mainly oriented in a northerly

and south-westerly direction.

The velocity data for the current profiler at the buoy have also been plotted according to wave heights (Fig. 8). These velocities are those that were registered in the whole water column during these specific periods but differ from the water particle velocity generated by the wave itself, which cannot be measured by such sensors. Nevertheless, it shows that during these time periods of high waves, the current velocity gradient was quite low in the first 14 m of the water column, which can indicate a good water mixing through this depth at the buoy location.

3.2. Oxygen, temperature and salinity variations

The temperatures data were extracted at two depths (5–12 m) from the oxygen sensors at the reference points and are shown in Fig. 9; salinity is shown in Fig. 10. It shows that the water column was well mixed.

All oxygen (DO) data were analyzed according to the statistical method presented in Section 2.4.1. The Spearman correlation coefficients (see Section 2.4.1) from this analysis are reported in Table 3. For each cage the DO data show a very strong correlation at 3 m and 5 m as the two depths are in the shielded water volume inside the skirt (to a depth of 7 m) surrounding the cages. In addition, cage 1 offers a very good correlation between all the three depths (3, 5, 12 m > 0.9), higher than the two other cages, which indicates that the water column in this cage was well mixed due to its location, very sheltered in comparison to the two other cages, and more exposed to currents. For the 12 m depth, cages 10 and 8 are correlated (>0.75) as these two cages experienced similar current speed, but no direct correlation could be seen between the two cages 10 (most exposed) and cage 1 (sheltered) as these two cages would be affected differently by both the currents and the waves.

3.3. Fish distribution

As explained in Section 2.4.2, the echosounders were analyzed using two different methods in order to capture the general behavior of the salmon during the wave periods. In Fig. 11, the vertical distribution for salmon in a heat map visualization is presented for all three cages and the three echosounders in each cage. These heat maps show that the behavior of the salmon in the monitored water column is different from cage to cage, depending on their exposure to waves and currents. The most exposed cage 10 shows a pattern of wave avoidance only in the upper part of the cage, while this effect is less marked for the two other cages, especially cage 1, which is the most sheltered. This observed wave avoidance at the surface can only be seen until a depth of a maximum of 3 m below the surface.

These echosounder data were further analyzed in order to detect any general trend in the behavior of the salmon in the monitored cage volume. In Fig. 12, the 50th percentile fish population (ref. Section 2.4.2) is represented for each cage and each echosounder, versus the increasingly

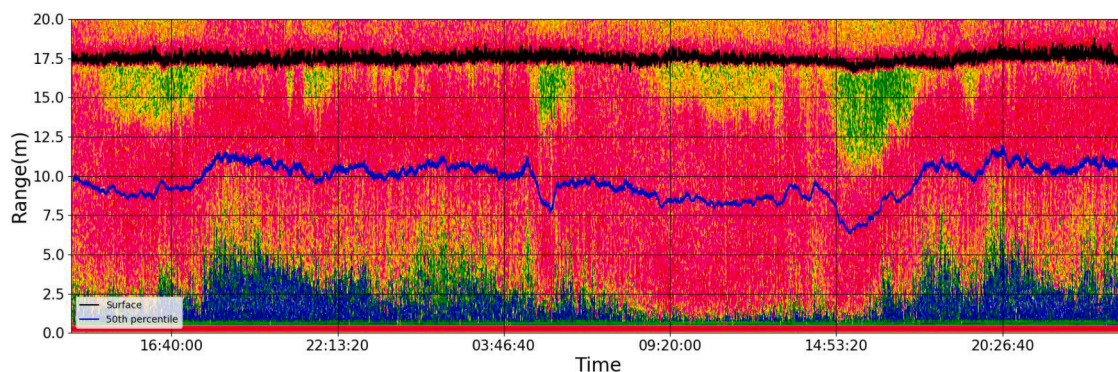


Fig. 4. Sample of raw data echosounder plot with estimated surface (black) and 50% fish population position (blue). The red pixel represents a strong signal from a target such as fish while blue pixel is associated to very low fish occurrence.

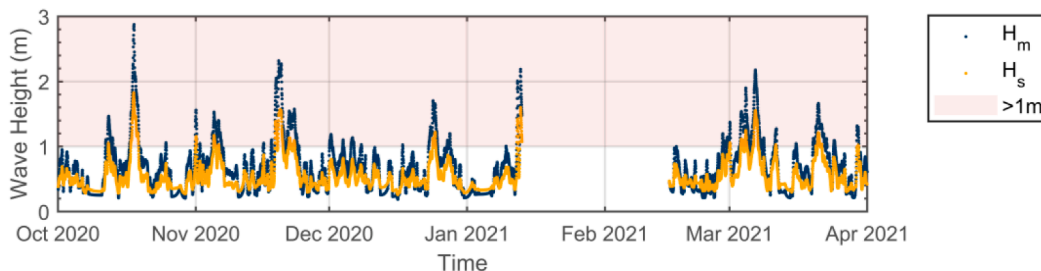


Fig. 5. Wave heights over time.

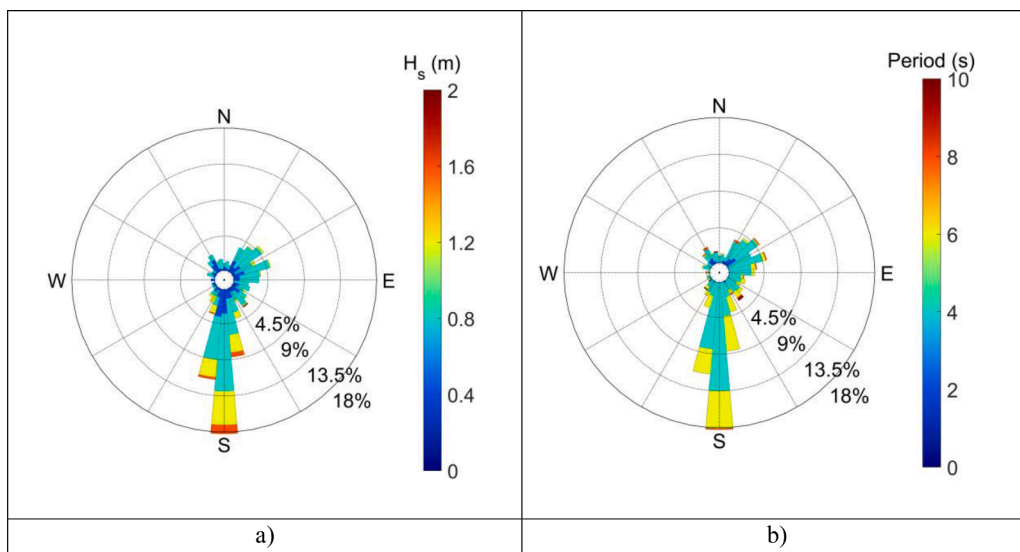


Fig. 6. Rose plots for (a) wave height and (b) wave period.

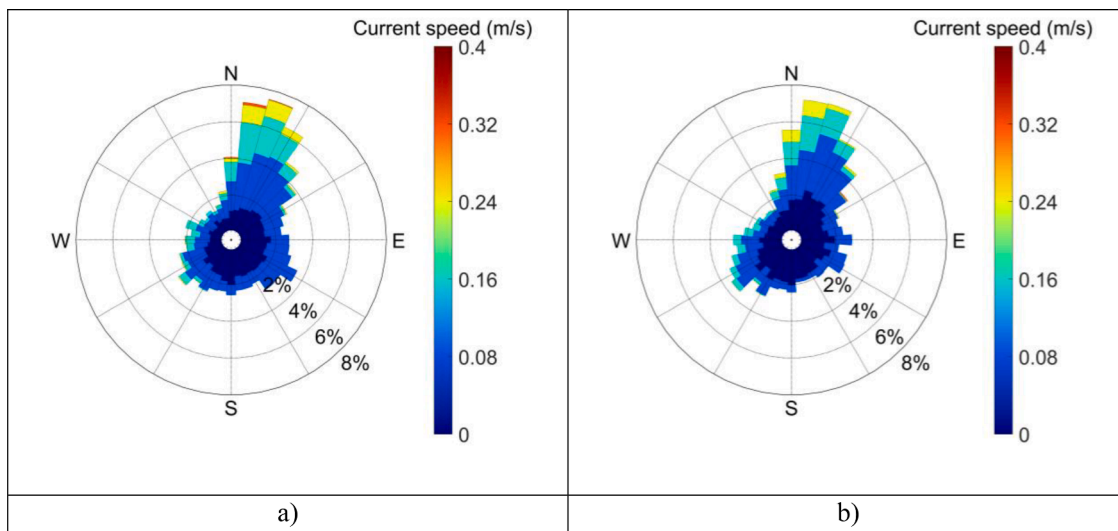


Fig. 7. Rose plot for current velocity at (a) 5 m (b) 11 m.

significant wave heights (H_s) measured at the site. From these analyses, it can be seen that in all cages the 50th percentile salmon population at the sides of the cages were mainly swimming at a depth of between six to seven meters with a slight preference for an upper depth on the north side in all the cages. The maximum available depth (cylindrical part) on the side of the cages was 12 m and the depth of the skirt was 7 m (from the surface). In the center of the cages, the 50th percentile salmon were

located deeper (8–9.5 m) than on the sides. Also, the echosounders were located at a lower depth (14–15 m). Salmon in cage 10 showed different behavior than the two other cages, as these were swimming at lower depths. From these plots it can be seen that the increasing waves did not noticeably affect the behavior of most of the salmon, as these mainly remained at their preferred swimming depths.

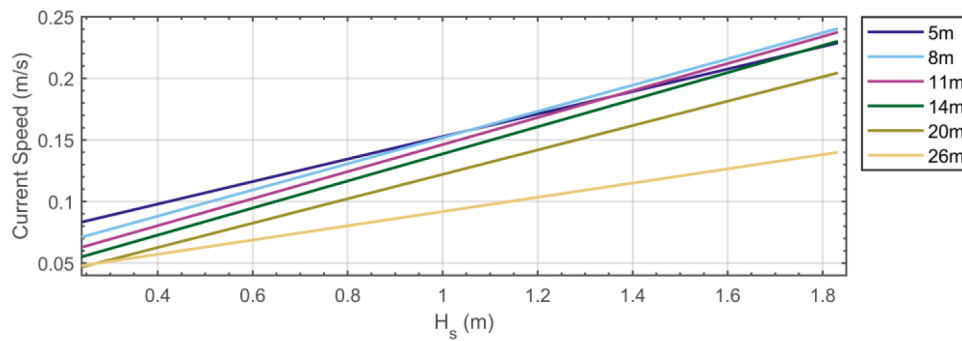


Fig. 8. Chart showing data of the relationship of current velocities, at different depths, with significant wave heights.

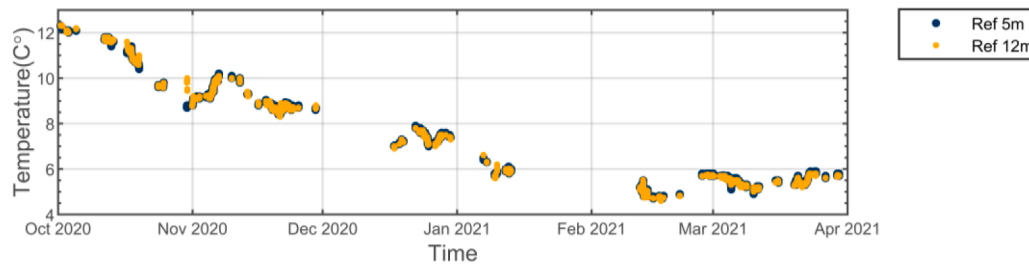


Fig. 9. Temporal variation of temperature at two different depths (5, 11 m) during high wave height.

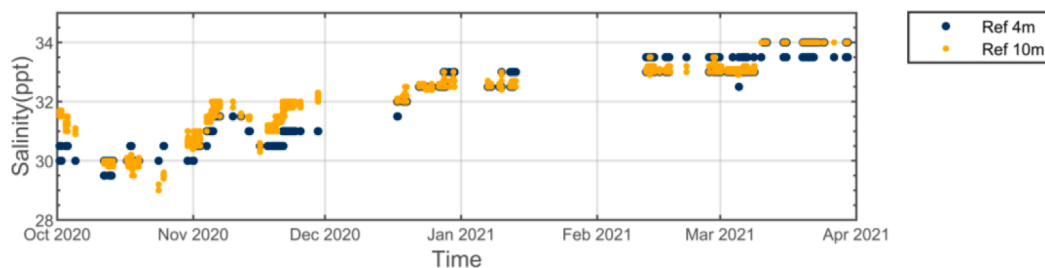


Fig. 10. Temporal variation of salinity at two different depths (5, 11 m) during high wave height.

Table 2

Equipment deployed during the measurements.

Type	Manufacturer	Specifications
Echosounders	Simrad	EK15 200 kHz 26° viewing angle
ADCP	NORTEK	Aquapro 400 kHz installed on the SeaWatch MIDI buoy from Fugro.
SeaWatch MIDI buoy	Fugro	Equipped with the following sensors: <ul style="list-style-type: none"> • Wavesense 3 (OCEANOR) • Compass (2.5PNI, TCM). • Air pressure (PTB330, Vaisala) • Air humidity and temperature.
Dissolved oxygen sensor	Aanderaa	Oxygen Optode 4531 inside the cages
Salinity sensor	Innovasea	Wireless optode-based sensors at the reference point.

4. Discussion

4.1. Correlation between fish distribution, waves and currents

The study site is classified, according to Table 1, as C-Medium for waves and A-Small for current categories. It is not expected that the cage has experienced high net deformation as a result of currents but mainly deformation of its floating collar due to waves: the estimated volume loss of the cage could be a maximum of 15%, as (Klebert et al., 2015)

measured a volume loss of 20% at 0.5 m/s.

The main difference in previous studies (Johannesen et al., 2022, 2020) conducted in the Faroe Islands is that the cages used in the current study are much deeper (standard cages used in Norway) than those used in the other studies. The observations from these previous studies are that there was a strong interaction between waves, currents and cage deformation that affected fish behavior. One of the main observations was that the salmon actively chose to occupy parts in the cage exposed to stronger currents but avoided the sea surface, if possible, when high waves were present; but this behavior was altered when high currents induced cage deformations, such as uplift of the bottom of the cage, which caused the fish to swim in the upper part of the water column and therefore in the waves.

In the current study, the behavioral response (swimming effort and mode) of the salmon to the waves and currents was not thoroughly studied in the same way as Johannesen et al. (2022, 2020) who deployed a large amount of optical (underwater cameras) and depth sensors. Instead, the focus was mainly on the shoal location with increasing wave heights and in cages with different levels of exposure, mainly to waves and currents, although the studied site is not classified as being exposed to currents.

From the environmental data parameters recorded on site, temperature, salinity and DO level were quite mixed in the water column, at least at the measured depths (to a depth of 12 m), so these could not affect the behavior of the salmon in the water column. Some differences

Table 3

Spearman correlation coefficients matrix. Bold numbers represent data from the same cage and a gray background represents data from the same depth. The interpretation of Spearman correlation coefficient are defined by (Weir, I., 2019): 0.00–0.19 “very weak”, 0.20–0.39 “weak”, 0.40–0.59 “moderate”, 0.60–0.79 “strong”, 0.80–1.0 “very strong”.

Variable	Cage 1 3 m	Cage 1 5 m	Cage 1 12 m	Cage 8 3 m	Cage 8 5 m	Cage 8 12 m	Cage 10 3 m	Cage 10 5m	Cage 10 12 m
Cage 1 3 m	1.00	0.90	0.93	0.65	0.51	0.78	0.63	0.72	0.52
Cage 1 5 m		1.00	0.87	0.69	0.46	0.73	0.73	0.74	0.43
Cage 1 12 m			1.00	0.60	0.46	0.76	0.56	0.69	0.52
Cage 8 3 m				1.00	0.85	0.73	0.85	0.76	0.72
Cage 8 5 m					1.00	0.71	0.65	0.62	0.76
Cage 8 12 m						1.00	0.68	0.76	0.75
Cage 10 3 m							1.00	0.83	0.69
Cage 10 5 m								1.00	0.67
Cage 10 12 m									1.00

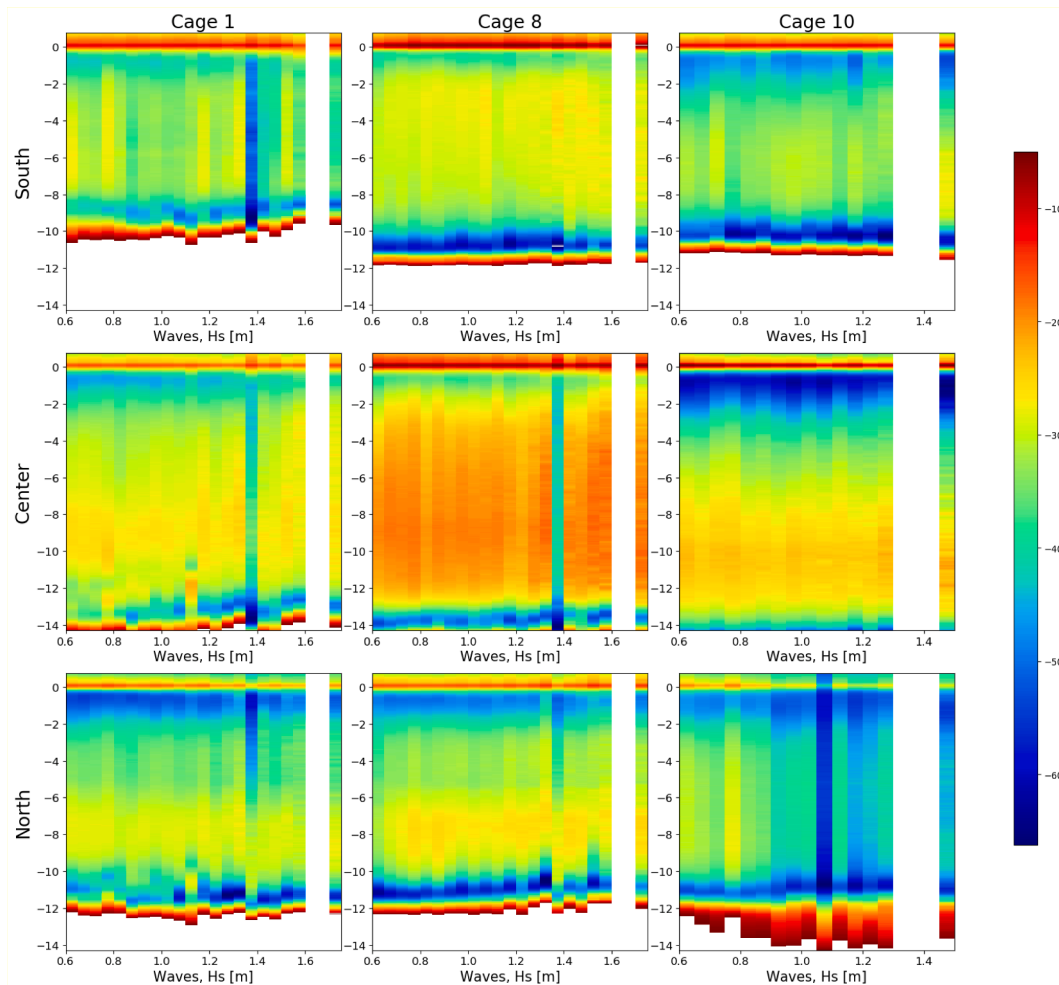


Fig. 11. Vertical distribution heat maps in the three studied cages for the three echosounders compared to wave height data (x-axis), where the y-axis represents the depth, and color intensity represents the average magnitude of the S_y data. It indicate fish occurrence, with higher values (−20) indicating many fish and lower values (−60) indicating fewer fish. The sea surface is at $y = 0$. The white vertical regions are periods during which there was a power outage during bad weather. In some plots, the sea surface and the very low depths areas are in red, these are only artifact signals.

in DO saturation, due to consumption by the salmon, were monitored in the three cages, and are related to their very different levels of exposure to waves and currents, but these are also unlikely to directly affect salmon behavior.

The current and wave data show that cage 10 experienced the most exposure to both currents and waves, while cage 1 is the most sheltered to both (Figs. 7 and 6). The analysis of the current profiles during the wave occurrences (Fig. 8) shows quite a mixed water column in the first 14 m. Also, due to the low main current velocity recorded (<0.25 m/s), it is unlikely that the salmon’s swimming mode was affected by these

current speeds with fish changing from swimming freely to standing on current as the current increased (Johansson et al., 2014).

The large amount of echosounder data have been analyzed using two different methods at all wave occurrences. From a heat map representation of the vertical distribution of the salmon in the monitored water columns (Fig. 11), it can be seen that different kinds of behavior occurred between the three cages. While in the most exposed cage (10), a wave avoidance occurred in the upper part (0–3 m) of the water column for the three echosounders (north, center and south side). This behavioral response was significantly less observed in the other cages (1

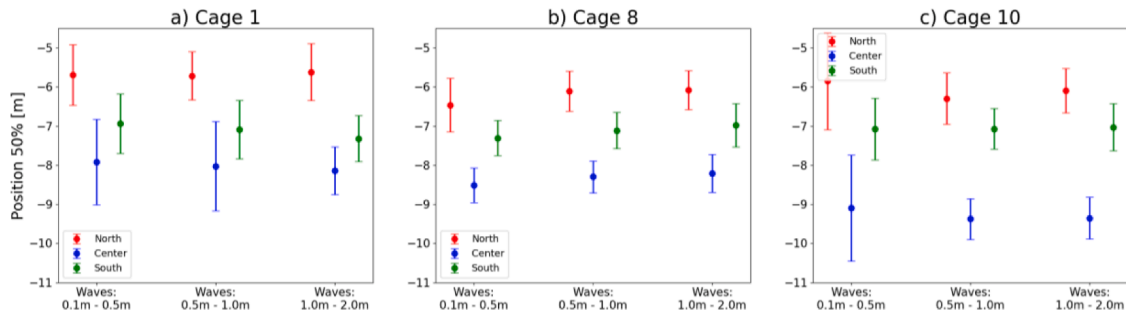


Fig. 12. Statistical analysis of the echosounder signal in each cage (a) cage 1, (b) cage 8, (c) cage 10 and for different wave heights considering 50% of the signal (50th percentile fish population).

and 8), most likely due to their lower exposure to waves. The echosounders on the north side of these cages showed a tendency to avoid increasing wave heights but minimal avoidance in the other positions. Another way of analyzing these data was to consider the location of the 50th percentile fish population at all the echosounder locations (Fig. 12) in order to more carefully monitor the behavior of the main population of salmon at these locations. From these plots, it can be seen, except at the center of the most exposed cage (10), that the main behavioral response of the salmon is that they were not noticeably affected by the effect of the waves at the surface.

4.2. Fish modeling

An in-house numerical tool (Reite et al., 2014; Su et al., 2019) was used in this study to simulate fish distributions in flexible sea cages with waves and currents. A thorough description and validation of the structural and hydrodynamic models for flexible sea cages can be found in (Klebert et al., 2015), (Endresen and Klebert, 2020) and (Su et al., 2021). An individual-based (Lagrangian) fish model ((Føre et al., 2009) has also been implemented for simulating the behavioral response of farmed salmon (*Salmo salar* L.) towards the cage, feed, temperature, light and other individuals. The implemented fish model is able to simulate full-scale fish populations (e.g., 200 000 individuals) in flexible sea cages in which the influence of hydrodynamic response and structural deformation is considered, as well as the influence of temperature, light and feed distributions in the cage.

To adapt the spatial response scheme to a more complex external environment, the fish model was expanded to include active responses to prevailing water currents (Johansson et al., 2014), and a simplified approach to simulate the effect of waves on fish has been introduced in this study. Herein, it is assumed that wave-induced water particle velocity and acceleration decreased with increased depth, according to the linear regular wave theory (Faltinsen, 1993):

$$\begin{cases} u(x, z, t) = \omega \xi_a e^{-kz} \sin(\omega t - kx) \\ w(x, z, t) = -\omega \xi_a e^{-kz} \cos(\omega t - kx) \end{cases} \text{ and } \begin{cases} a_1(x, z, t) = \omega^2 \xi_a e^{-kz} \cos(\omega t - kx) \\ a_2(x, z, t) = \omega^2 \xi_a e^{-kz} \sin(\omega t - kx) \end{cases}$$

where x is the horizontal coordinate in the wave propagation direction, z

is the vertical coordinate (positive downwards), t is the time variable, ω is the wave frequency ($2\pi/T$, T = wave period), ξ_a is the wave amplitude and k is the wave number ($2\pi/\lambda$, λ = wavelength).

Fig. 13 shows three examples of the calculated average amplitudes of water particle velocity and acceleration at different depths. According to this model, the velocity and the acceleration are also dependent on wave periods, not only amplitudes.

In the simulation case study, a simple avoidance criterion was applied for the fish to move downwards from the depth where either the water particle velocity (average amplitude) was higher than 0.3 m/s or the water particle acceleration (average amplitude) was higher than 0.4 m/s². No direct reference was found for the avoidance criterion towards waves, it was just set according to the present field observations without considering the possible effects of fish size. The mean weight of the simulated fish was 2 kg, the number of simulated fish was 160 000, and it was assumed that the fish preferred to occupy the entire cage volume. As shown in Fig. 14, the simulation model is able to reproduce the observed fish distributions in currents and waves, i.e., farmed salmon actively chose to move towards the upstream side (from where the current flows) of the cage and avoid the surface when high waves were present (Johannesen et al., 2022). Different simulation cases are conducted with two current velocities (0.1–0.3 m/s) and two wave periods (6–8 s) to illustrate the effect of these parameters using the same wave heights (2.5 m).

The simulation case study was only intended to demonstrate the potential of an existing fish model for reproducing the present field observations. More quantitative data are needed for parameterization and verification of the extended fish behavioral expressions towards currents, waves and the resulting cage responses/deformations.

5. Conclusion

The field measurements reported in this study shed new light on the behavioral response of Atlantic salmon to waves. While recent studies have shown that strong waves and currents reduce the available space for farmed salmon in a sea cage (cf. Section 4), thereby affecting their behavior, the present study shows that the behavior of salmon in waves is dependent on the location of the cage relative to the farm layout, and

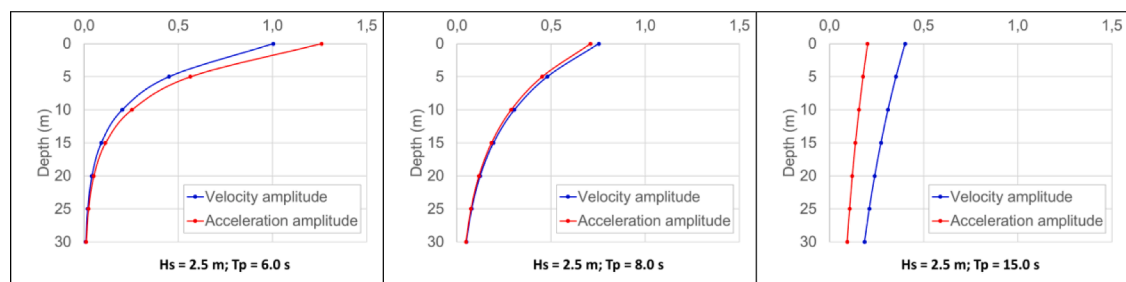


Fig. 13. Examples of the calculated average amplitudes of water particle velocity (m/s) and acceleration at different depths (m/s²) in the x-axis.

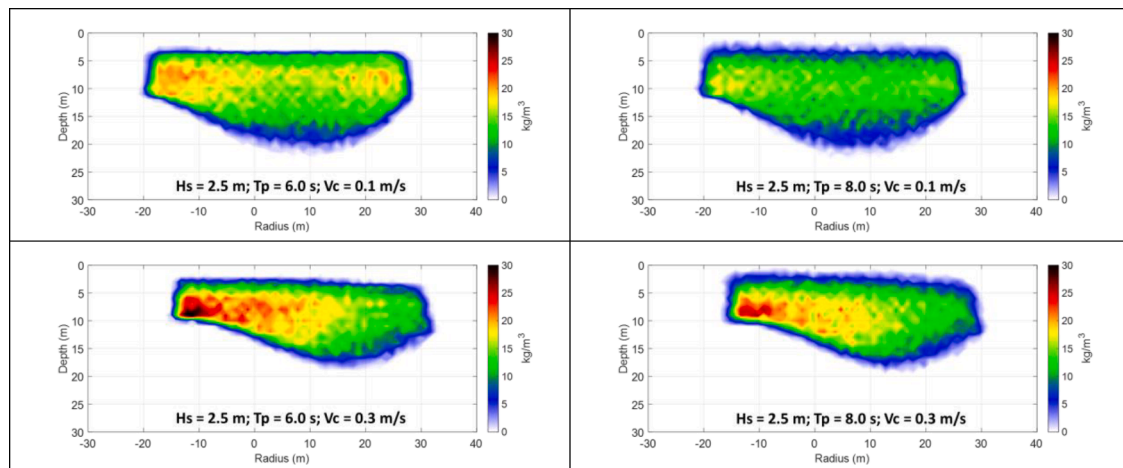


Fig. 14. Examples of the simulated fish distributions in a flexible sea cage with currents and waves. Colormap indicates directly the fish density (from 0–30 kg/m³).

this is limited to the upper part of the water column. In general, if cages do not experience large deformations as a result of high currents and if they are deep enough, the waves would only trigger an avoidance behavior in the first few meters (e.g., 0–3 m) under the water surface while the main population in the water column are largely unaffected. This could be attributed to the fact that the water particle velocity and acceleration generated by the waves decrease with increased depth, as well as the resulting cage responses. A relevant avoidance criterion has been implemented for the simulation of fish behavior in waves, based on an integrated numerical model of fish and a flexible sea cage. It was found that the simulation model was able to reproduce the observed fish distributions in general. However, more data are needed for parameterization and verification of this extended behavioral expressions.

Authors statement

Pascal Klebert: Conceived and designed the experiments, performed the experiments, analyzed the data and Supervision, Writing- Original draft, Methodology.

Biao Su: Modelling, Writing- Reviewing and Editing.

Oscar Nissen and Bjarne Kvæstad: formal analysis, Visualization, writinf - review & editing.

Declaration of Competing Interest

The authors declare that they have no known competing financial interests or personal relationships that could have appeared to influence the work reported in this paper.

Data availability

Data will be made available on request.

Acknowledgements

This study presented in this paper was carried out as part of a research project from the RACE research grant program funded by SINTEF OCEAN and through the Centre for Research-Based Innovation on exposed aquaculture operations (SFI EXPOSED: 237790/O30) led by SINTEF OCEAN and funded by the Research Council of Norway.

References

Elliott, J.M., Elliott, J.A., 2010. Temperature requirements of Atlantic salmon *Salmo salar*, brown trout *Salmo trutta* and Arctic charr *Salvelinus alpinus*: predicting the

- effects of climate change. *J. Fish Biol.* 77, 1793–1817. <https://doi.org/10.1111/j.1095-8649.2010.02762.x>.
- Endresen, P.C., Klebert, P., 2020. Loads and response on flexible conical and cylindrical fish cages: a numerical and experimental study based on full-scale values. *Ocean Eng.* 216, 107672 <https://doi.org/10.1016/j.oceaneng.2020.107672>.
- Faltinsen, O., 1993. *Sea Loads On Ships and Offshore Structures*. Cambridge University Press.
- Føre, M., Dempster, T., Alfredsen, J.A., Johansen, V., Johansson, D., 2009. Modelling of Atlantic salmon (*Salmo salar* L.) behaviour in sea-cages: a Lagrangian approach. *Aquaculture* 288, 196–204. <https://doi.org/10.1016/j.aquaculture.2008.11.031>.
- Bjelland, H.V., Føre, M., Lader, P., Kristiansen, D., Holmen, I.M., Fredheim, A., G. røtli, E.I., F.athi, D.E., Oppedal, F., U.tne, I.B., Schjølberg, I., 2015. Exposed Aquaculture in Norway. In: Presented at the OCEANS 2015. Washington. MTS/IEEE, pp. 1–10. <https://doi.org/10.23919/OCEANS.2015.7404486>.
- Harris, C.R., Millman, K.J., van der Walt, S.J., Gommers, R., Virtanen, P., Cournapeau, D., Wieser, E., Taylor, J., Berg, S., Smith, N.J., Kern, R., Picus, M., Hoyer, S., van Kerkwijk, M.H., Brett, M., Haldane, A., del Río, J.F., Wiebe, M., Peterson, P., Gérard-Marchant, P., Sheppard, K., Reddy, T., Weckesser, W., Abbasi, H., Gohlke, C., Oliphant, T.E., 2020. Array programming with NumPy. *Nature* 585, 357–362. <https://doi.org/10.1038/s41586-020-2649-2>.
- Holmer, M., 2010. Environmental issues of fish farming in offshore waters: perspectives, concerns and research needs. *Aquac. Environ. Interact.* 1, 57–70.
- Hvas, M., Folkedal, O., Oppedal, F., 2021. Fish welfare in offshore salmon aquaculture 13, 836–852. <https://doi.org/10.1111/raq.12501>.
- Hvas, M., Folkedal, O., Solstorm, D., Vågseth, T., Fosse, J.O., Gansel, L.C., Oppedal, F., 2017. Assessing swimming capacity and schooling behaviour in farmed Atlantic salmon *Salmo salar* with experimental push-cages. *Aquaculture* 473, 423–429. <https://doi.org/10.1016/j.aquaculture.2017.03.013>.
- Hvas, M., Oppedal, F., 2017. Sustained swimming capacity of Atlantic salmon. *Aquacul. Environ. Interact.* 9, 361–369.
- Johannesen, A., Patursson, O., Kristmundsson, J., Dam, S.P., Klebert, P., 2020. How caged salmon respond to waves depends on time of day and currents. *PeerJ* 8. <https://doi.org/10.7717/peerj.9313>.
- Johannesen, A., Patursson, Ø., Kristmundsson, J., Dam, S.P., Mulelid, M., Klebert, P., 2022. Waves and currents decrease the available space in a salmon cage. *PLoS ONE* 17, e0263850. <https://doi.org/10.1371/journal.pone.0263850>.
- Johansson, D., Laursen, F., Fernö, A., Fosseidengen, J., Klebert, P., Stien, L.H., Tone, V., Frode, O., 2014. The interaction between water currents and salmon swimming behaviour in sea cages. *PLoS ONE* 9 (5), e97635. <https://doi.org/10.1371/journal.pone.0097635>.
- Johansson, D., Ruohonen, K., Kiessling, A., Oppedal, F., Stiansen, J.-E., Kelly, M., Juell, J.-E., 2006. Effect of environmental factors on swimming depth preferences of Atlantic salmon (*Salmo salar* L.) and temporal and spatial variations in oxygen levels in sea cages at a fjord site. *Aquaculture* 254, 594–605. <https://doi.org/10.1016/j.aquaculture.2005.10.029>.
- Klebert, P., Lader, P., Gansel, L., Oppedal, F., 2013. Hydrodynamic interactions on net panel and aquaculture fish cages: a review. *Ocean Eng.* 58, 260–274. <https://doi.org/10.1016/j.oceaneng.2012.11.006>.
- Klebert, P., Patursson, Ø., Endresen, P.C., Rundtop, P., Birkevold, J., Rasmussen, H.W., 2015. Three-dimensional deformation of a large circular flexible sea cage in high currents: field experiment and modeling. *Ocean Eng.* 104, 511–520. <https://doi.org/10.1016/j.oceaneng.2015.04.045>.
- Lader, P., Kristiansen, D., Alver, M., Bjelland, H.V., Myrhaug, D., 2017. Classification of aquaculture locations in norway with respect to wind wave exposure. In: Presented at the ASME 2017 36th International Conference on Ocean, Offshore and Arctic Engineering. <https://doi.org/10.1115/omae2017-61659>. V006T05A005.
- MATLAB and Statistics Toolbox Release, 2020. The MathWorks, Inc., Natick, Massachusetts, United States n.d.
- McIntosh, P., Barrett, L.T., Warren-Myers, F., Coates, A., Macaulay, G., Szetey, A., Robinson, N., White, C., Samsing, F., Oppedal, F., Folkedal, O., Klebert, P.,

- Dempster, T., 2022. Supersizing salmon farms in the coastal zone: a global analysis of changes in farm technology and location from 2005 to 2020. *Aquaculture* 553, 738046. <https://doi.org/10.1016/j.aquaculture.2022.738046>.
- McKinney, W., 2010. Data structures for statistical computing in Python. In: Walt, S. van der, Millman, J. (Eds.), *Proceedings of the 9th Python in Science Conference*, pp. 56–61. <https://doi.org/10.25080/Majora-92bf1922-00a>.
- Morro, B., Davidson, K., Adams, T.P., Falconer, L., Holloway, M., Dale, A., Aleynik, D., Thies, P.R., Khalid, F., Hardwick, J., Smith, H., Gillibrand, P.A., Rey-Planellas, S., 2021. Offshore aquaculture of finfish: big expectations at sea. *Rev. Aquac.* 1–25. <https://doi.org/10.1111/raq.12625> n/a.
- Noble, C., Gismervik, K., Iversen, M.H., Kolarevic, J., Nilsson, J., Stien, L.H., Turnbull, J. F., 2018. Welfare Indicators for farmed Atlantic salmon: tools for assessing fish welfare.
- Oppedal, F., Dempster, T., Stien, L.H., 2011. Environmental drivers of Atlantic salmon behaviour in sea-cages: a review. *Aquaculture* 311, 1–18. <https://doi.org/10.1016/j.aquaculture.2010.11.020>.
- Puth, M.-T., Neuhäuser, M., Ruxton, G.D., 2015. Effective use of Spearman's and Kendall's correlation coefficients for association between two measured traits. *Anim. Behav.* 102, 77–84. <https://doi.org/10.1016/j.anbehav.2015.01.010>.
- Reite, K.-J., Føre, M., Aarsæther, K.G., Jensen, J., Rundtop, P., Kyllingstad, L.T., Endresen, P.C., Kristiansen, D., Johansen, V., Fredheim, A., 2014. Fhsim—Time domain simulation of marine systems. In: *International Conference on Offshore Mechanics and Arctic Engineering*. American Society of Mechanical Engineers. V08AT06A014.
- Remen, M., Solstorm, F., Bui, S., Klebert, P., Vågseth, T., Solstorm, D., Hvas, M., Oppedal, F., 2016. Critical swimming speed in groups of Atlantic salmon *Salmo salar*. *Aquacult. Environ. Interact.* 8, 659–664. <https://doi.org/10.3354/aei00207>.
- Solstorm, F., Solstorm, D., Oppedal, F., Olsen, R., Stien, L., Fernö, A., 2016. Not too slow, not too fast: water currents affect group structure, aggression and welfare in post-smolt Atlantic salmon *Salmo salar*. *Aquac. Environ. Interact.* 8, 339–347. <https://doi.org/10.3354/aei00178>.
- Standard Norge, 2009. NS 9415:2009 Marine fish farms. Requirements for desing, dimensioning, production, installation and operation. *Norsk Standard*. NS 9415.
- Stien, L.H., Lind, M.B., Oppedal, F., Wright, D.W., Seternes, T., 2018. Skirts on salmon production cages reduced salmon lice infestations without affecting fish welfare. *Aquaculture* 490, 281–287. <https://doi.org/10.1016/j.aquaculture.2018.02.045>.
- Su, B., Kelasidi, E., Frank, K., Haugen, J., Føre, M., Pedersen, M.O., 2021. An integrated approach for monitoring structural deformation of aquaculture net cages. *Ocean Eng.* 219, 108424 <https://doi.org/10.1016/j.oceaneng.2020.108424>.
- Su, B., Reite, K.-J., Føre, M., Aarsæther, K.G., Alver, M.O., Endresen, P.C., Kristiansen, D., Haugen, J., Caharija, W., Tsarau, A., 2019. A multipurpose framework for modelling and simulation of marine aquaculture systems. In: *Ocean Space Utilization*, 6. <https://doi.org/10.1115/OMAE2019-95414>.
- Van Rossum, G., Drake, F.L., 2009. Python 3 reference manual. CreateSpace.
- Wall, C.C., Towler, R., Anderson, C., Cutter, R., Jech, J.M., 2018. PyEcholab: an open-source, python-based toolkit to analyze water-column echosounder data. *J. Acoust. Soc. Am.* 144, 1778. <https://doi.org/10.1121/1.5067860>. –1778.
- Weir, I., 2019. Spearman's Correlation. Available online: <https://www.statstips.com/spearman-correlation/>.